

# Vertical Distribution of Primary Production and Chlorophyll a in the Kara Sea

A. B. Demidov and S. A. Mosharov

*Shirshov Institute of Oceanology, Russian Academy of Sciences, ul. Krasikova 23, Moscow, 117218 Russia*

*e-mail: demspa@rambler.ru*

Received March 20, 2014

**Abstract**—On the basis of data obtained during three ecosystem expeditions in the Kara Sea, the vertical variability of the primary production (PP) and chlorophyll a (Chl) in autumn was studied. The Chl maximum was detected mainly on the surface ( $Chl_0$ ). A homogenous Chl distribution in the euphotic layer (1% photosynthetically available radiation) and a nearly linear decrease in the Chl concentration below this layer were observed in waters with  $Chl_0$  values of 0.1–0.5 mg/m<sup>3</sup>. In waters with  $Chl_0 > 0.5$  mg/m<sup>3</sup>, the Chl concentration in the studied layer decreased linearly or exponentially. The subsurface Chl maximum (SCM) was registered weekly and was detected mostly in waters with a  $Chl_0$  content of 0.1–0.5 mg/m<sup>3</sup>. The SCM formation in the Kara Sea was consistent with the general patterns for the World Ocean. Water-column stability, the content of biogenic elements, and the level of subsurface irradiance had an approximately equal effect on SCM formation. The contribution of the SCM to the depth-integrated PP varied from 1 to 27%. The parameterization of vertical profiles of Chl was performed in order to be used in depth-integrated PP models. The Chl maximum on the surface and the negligible SCM facilitate the estimation of depth-integrated PP on the basis of satellite data and the use of vertical-resolution models.

DOI: 10.1134/S0001437015040025

## INTRODUCTION

Satellite monitoring over the past four decades has been one of the main methods to monitor the spatiotemporal variability of biogeochemical parameters of the ocean surface. The standpoint that a large-scale assessment of the level of productivity of marine ecosystems is only possible with the use of satellite data has become an axiom. However, the interpretation of and approaches to the use of remote sensing with the aid of ocean color scanners must be improved. For example, the development of models of primary production in the water column on the basis of bio-optical data obtained for the subsurface layer of the ocean and their subsequent verification remains a topical problem [13, 14, 23, 46, 47]. Key tasks include studies of phytoplankton production indices on the surface and in the water column, as well as the identification of the pattern of their vertical distribution. In contrast to surface indices, features of vertical changes in production indices can be studied only under field conditions.

When assessing primary production in the water column ( $PP_{\text{phs}}$ ), it is important to know the extent to which data on surface Chl content ( $Chl_0$ ) characterize the content of this pigment in the entire photosynthetic layer and determine the type of its vertical distribution. The principles of interpretation of data on the surface Chl content are based on the conclusion that the  $Chl_0$  concentration, first, is closely related to a depth-integrated value in the photosynthetic layer ( $Chl_{\text{phs}}$ ) and, secondly, determines the shape of the curve illustrating

the vertical distribution of Chl. The latter is characterized by the presence, degree of expression, or absence of the subsurface Chl maximum (SCM) and depends on the trophic status of waters if  $Chl_0$  concentration is taken as an index [36, 53].

A subsurface Chl maximum is a characteristic element of the curve of the vertical distribution of Chl in stratified waters [18]. Its genesis is associated with phytoplankton concentration in the layer of maximum pycnocline gradients in late spring and summer after the spring bloom sinks to a lower depth [50] as well as with an increase in the Chl content in cells, which is associated with the chromatic adaptation of the shade-tolerant nutricline population to an irradiance still sufficient for photosynthesis [30]. The presence of SCM hampers the assessment of  $PP_{\text{phs}}$  on the basis of satellite data obtained only from the surface layer of the ocean. In the Arctic seas, the structure, function, and value of the SCM has been studied mainly in the western sector of the region [15, 17, 25, 39]. Recently, the patterns of the formation and variability of the SCM have been studied and its effect on the annual integrated primary production for all the seas of the Arctic estimated [8, 9].

It should be noted that the vertical distribution of Chl and primary production (PP) were studied, and conclusions on the correlation between  $Chl_0$  content and values in the water column and types of curves were made for the waters of the so-called first optical type (Case I), the characteristics of which are formed mostly

by the autochthonous substance (primarily phytoplankton) [24, 31]. The Kara Sea is classified with water bodies of the second optical type (Case II), whose optical properties are formed primarily under the influence of allochthonous particulate and dissolved organic matter and terrigenous mineral suspension [1, 4]. Studies of the characteristics of the vertical distribution of the phytoplankton production indices in the Arctic seas with this water type have not been performed before the current time. For this reason, vertical changes in Chl and PP and the values of the abiotic factors that determine them in the Kara Sea are the least studied [11, 27]. Earlier studies were focused only on the descriptions of the vertical variability of these indices on section in different parts of the sea [3, 5].

The objectives of this study were (1) to distinguish the types of vertical distribution of PP and Chl in the Kara Sea depending on the abiotic factors (the subsurface irradiance level, the content of basic biogenic elements, and water column stability); (2) to assess the contribution of different layers of the water column to the integrated values of Chl and PP; (3) to identify the dependence of SCM formation on abiotic factors; and (4) to perform averaging and mathematical approximation of the curves of the vertical distribution of Chl in waters of different trophic types.

## MATERIALS AND METHODS

**Data sources and distinguishing water areas with different trophic status.** The database analyzed in this work was created from results of three complex ecosystem expeditions to the Kara Sea: the 49th voyage of the RV *Dmitrii Mendeleev* (August–September 1993) and the 54th and 59th voyages of the RV *Akademik Mstislav Keldysh* (September 2007 and September–October 2011, respectively). The summary description of the study area and location of stations were given in a previous paper [19]. The total Chl content was studied at 113 stations, and primary production was measured at 85 stations.

On the basis of the available data set, the vertical profiles of Chl, primary production, and abiotic factors (subsurface irradiance in the range of photosynthetically active radiation (PAR), water density ( $\sigma_t$ ), and the amount of nitrite and nitrate nitrogen ( $\text{NO}_2 + \text{NO}_3$ )) were distributed according to trophic types. Chl content on the surface ( $\text{Chl}_0$ ) in the ranges 0.1–0.5 (I), 0.5–1.0 (II), 1.0–2.0 (III), and > 2 (IV)  $\text{mg}/\text{m}^3$  was chosen as an index of water productivity [36, 53].

As noted in previous studies describing the vertical distribution of Chl, stratified and unstratified waters should be considered separately [36, 53]. In these studies, the ratio of the thickness of the photosynthetic layer ( $H_{\text{phs}}$ ) to the thickness of the upper mixed layer (UML) ( $H_{\text{phs}}/\text{UML}$ ) served as a criterion of water stratification. Waters with  $H_{\text{phs}}/\text{UML} > 1$  were considered stratified, and waters with  $H_{\text{phs}}/\text{UML} < 1$  were considered well mixed. In autumn, when our studies

were performed, the majority of water areas in the Kara Sea were characterized by a sharp pycnocline in the upper 10-m layer ( $\text{UML} = 7\text{--}10$  m). The thickness of the photosynthetic layer usually exceeded UML thickness and averaged between 6 and 47 m in different parts of the sea [19]. Therefore, we decided to include all examined waters in the stratified type and classify vertical profiles of PP and Chl only by trophic types.

**Sampling and methods for determination of primary production and chlorophyll content.** The location of stations was chosen on the basis of the results of hydrophysical and hydro-optical surveys, which were performed using the Rybka multiparametric scanning probe and a flow fluorometer developed at the Institute of Oceanology, Russian Academy of Sciences. Sampling horizons were determined after preliminary probing the temperature, conductivity, and fluorescence with SBE-19 and SBE-32 CTD probes (Seabird Electronics).

To determine Chl content, water samples were collected with plastic bathometers of the Carousel Water Sampler complex from six to nine horizons of the upper 100-m layer. The sample from the subsurface layer at these stations was taken with a plastic bucket simultaneously with the closure of bathometers near the surface.

On the 49th voyage of the RV *Dmitrii Mendeleev*, PP in three stations was measured in situ. In other stations, PP was determined using a sample from the surface, vertical profiles of Chl and subsurface irradiance, and light curves obtained in situ. On the 54th voyage of the *Akademik Mstislav Keldysh* (2007), samples for PP determination were collected from the horizons with irradiance of 100, 75, 50, 25, 10, 5, and 2% of the subsurface irradiance in the PAR range ( $I_0$ ). On the 59th voyage of the RV *Akademik Mstislav Keldysh* (2011), sampling was performed from the horizons in which light conditions approximately corresponded to the nominal transmittance of flasks with neutral density filters of the following percentages of  $I_0$ , namely: 100, 78.7, 63.9, 48.7, 24.3, 5.8, 3.2, and 2.2; these filters came with the ICES laboratory incubator.

On all expeditions, PP was measured by radiocarbon modification of the flask method [49] using different experimental schemes [19]. Chl content was determined spectrophotometrically [33, 48] or fluorometrically [29, 32].

**Methods for the determination of surface and subsurface irradiance and hydro-chemical indicators.** The intensity of surface irradiance was measured with a pyranometer [3] or an LI-190SA incident radiation sensor (LI-COR) in the PAR range. Measurement results were automatically integrated into the LI-1400 unit at 5-min intervals ( $\text{Ein}/\text{m}^2$ ) during the day and were stored in the internal memory unit. Subsequently, these values were used to calculate integrated incident radiation for the period of exposure of the experimental flasks in determining PP and for the entire light period for a certain date.

The index of vertical attenuation of irradiance ( $k_d$ ) was measured using an alpha meter. In the absence of subsurface hydro-optical measurements,  $k_d$  values were calculated by the empirical dependence of the diffuse light attenuation from relative transparency by Secchi depth, which was obtained in August–September 1993 [19].

Samples for the determination of pH, biogenic elements (silicates, phosphates, and nitrogen forms), and alkalinity were collected into 0.5-L plastic flasks without preservatives. When working with waters abounding in particulate matter (water in the estuaries in the zone of mixing of river and sea waters), samples for determination of biogenic elements were preliminarily filtered through a lavsan nuclear filter (mesh, 1  $\mu\text{m}$ ) manufactured at the Joint Institute for Nuclear Research (Dubna). In samples with a visually noticeable color of water, colorimetric determination of mineral phosphorus and silicates was performed by the appropriate procedure [6, 7].

The total titratable alkalinity (Alk) was determined by direct titration according to Bruevich with a visual determination of the titration end point [7]. Dissolved inorganic and total phosphorus (phosphates), dissolved inorganic silicon (silicates), nitrite nitrogen (nitrites), nitrate nitrogen (nitrates), and ammonium nitrogen (ammonium ion) were determined colorimetrically, as described in [6, 7].

The content of dissolved carbon dioxide and various forms of dissolved inorganic carbon was calculated by the pH-Alk method according to thermodynamic equations of carbonate equilibrium using the Roy concentration dissociation constants of carbonic acid [35] with correction for waters whose properties differed from the properties of seawater [2, 34].

**Statistical analysis and parameterization of the vertical profiles of primary production and chlorophyll.** The vertical profiles of PP and Chl were averaged within each trophic type for 5-m layers in the upper 55-m water column. The averaged profiles in waters with different productivity were compared by the double normalization method, according to which the distribution of  $PP_z/PP_m$  and  $Chl_z/Chl_m$  was considered in relation to the optical depths ( $\zeta = Zk_d$ ), where  $Z$  is the geometrical depth,  $PP_z$  and  $Chl_z$  are PP and Chl values at depth  $Z$ , and  $PP_m$  and  $Chl_m$  are their maximum values in the water column [27].

Vertical profiles were approximated by the Gaussian curve, which is often used to describe the curve of the vertical distribution of Chl [44]. This approach was used, in particular, to calculate SCM thickness:

$$H = h/\sigma\sqrt{2\pi},$$

where  $H$  is the Chl concentration in the maximum layer,  $h$  is the integrated Chl content in the study layer, and  $\sigma$  is maximum thickness of Chl. Therefore,

$$\sigma = h/H\sqrt{2\pi}.$$

The SCM was regarded as well-expressed if the ratio of the concentration of Chl in the maximum layer to its concentration on the surface ( $Chl_m/Chl_0$ ) was  $\geq 1.15$  [53].

A value exceeding the photosynthetic layer by 1.5 times ( $1.5H_{\text{phs}}$ ) was conditionally taken as the lower limit of the study layer [53]. In addition, to assess the contribution to the integrated Chl values, we selected a layer forming the signal for the satellite color scanner ( $Z = 1/k_d$ ) and the UML. The lower limit of the UML was determined visually by  $\sigma_t$  curves. The difference between  $\sigma_t$  at depths of 0 and 20 m ( $\Delta\sigma_t = \sigma_{t,20} - \sigma_{t,0}$ ) was used as an index of water-column stability. A depth of 20 m was selected as the horizon laying under the maximum gradient layer, below which water density usually increased insignificantly. It should be noted that in deep-water areas of the Arctic Ocean  $\Delta\sigma_t$  was calculated using the layer of 0–80 m [51].

## RESULTS

**Characteristics of water areas of different trophic levels.** The waters of trophic types I and II (see above) include primarily water areas in the western and eastern slopes of the St. Anna Trough and in the southwestern part of the Kara Sea. The waters of trophic types III and IV occupy the area under the influence of the river flow as well as the Ob and Yenisei estuaries [19].

Tables 1 and 2 summarize the statistical indices of production characteristics of phytoplankton and abiotic factors for the waters of different trophic levels of the Kara Sea. Average PP and Chl values naturally increased as the concentration of surface Chl increased. This trend was less pronounced for the integrated Chl values in the photosynthetic layer ( $Chl_{\text{phs}}$ ) and in the study layer ( $Chl_{1.5\text{phs}}$ ). For the last two parameters, a significant (2.4–2.7-fold) increase was observed only upon the transition from type III to type IV (Table 1). This pattern can be explained by a decrease in the photosynthetic layer with an increase in the Chl content on the surface and in the water column.

As the productivity of water areas increased, the values of optical parameters characterizing the water layer decreased (Table 2). The mean values of phosphates ( $PO_{4\text{av}}$ ), dissolved silica  $Si(OH)_{4\text{av}}$ , and ammonium nitrogen ( $NH_{4\text{av}}$ ) increased with increases in the  $Chl_0$  content. Conversely, the content of the sum of nitrite and nitrate nitrogen did not change significantly during the transition from water of type I to type IV (Table 2). The thickness of the upper mixed layer remained virtually unchanged in the waters of trophic types I–IV. The water column stability index  $\Delta\sigma_t$  was 1.3–1.5 times lower in waters with a  $Chl_0$  content of 0.1–0.5  $\text{mg}/\text{m}^3$  as compared to more productive areas (Table 2).

**Vertical distribution of chlorophyll and primary production.** The characteristic curves of the vertical distribution of Chl, PP, the sum of nitrite and nitrate nitrogen, and water density are shown in Figs. 1 and 2. In the areas where it was not possible to find a well-

**Table 1.** Values of the production characteristics of phytoplankton in Kara Sea waters of different trophic levels

Index	Trophic level			
	0.1–0.5	0.5–1.0	1.0–2.0	>2.0
Chl <sub>0</sub>	$\frac{0.37 \pm 0.1}{25}$	$\frac{0.74 \pm 0.12}{30}$	$\frac{1.35 \pm 0.21}{36}$	$\frac{3.39 \pm 1.13}{20}$
Chl <sub>phs</sub>	$\frac{13.05 \pm 6.53}{21}$	$\frac{11.57 \pm 6.69}{22}$	$\frac{12.56 \pm 6.88}{24}$	$\frac{30.40 \pm 14.90}{17}$
Chl <sub>Z</sub>	$\frac{1.73 \pm 0.38}{24}$	$\frac{2.34 \pm 0.53}{29}$	$\frac{2.89 \pm 0.90}{32}$	$\frac{5.61 \pm 2.20}{19}$
Chl <sub>UML</sub>	$\frac{3.27 \pm 1.57}{24}$	$\frac{5.09 \pm 2.57}{29}$	$\frac{8.02 \pm 4.66}{32}$	$\frac{33.03 \pm 28.56}{19}$
Chl <sub>1.5phs</sub>	$\frac{16.21 \pm 7.51}{21}$	$\frac{13.27 \pm 7.82}{20}$	$\frac{14.76 \pm 7.74}{24}$	$\frac{39.33 \pm 22.90}{16}$
PP <sub>0</sub>	$\frac{4.41 \pm 2.72}{21}$	$\frac{6.36 \pm 4.70}{22}$	$\frac{24.08 \pm 47.18}{24}$	$\frac{53.28 \pm 31.26}{17}$
PP <sub>phs</sub>	$\frac{40 \pm 23}{21}$	$\frac{43 \pm 36}{22}$	$\frac{60 \pm 46}{24}$	$\frac{142 \pm 109}{17}$
PP <sub>Z</sub>	$\frac{17 \pm 11}{21}$	$\frac{17 \pm 16}{22}$	$\frac{28 \pm 23}{24}$	$\frac{76 \pm 52}{16}$
PP <sub>UML</sub>	$\frac{23 \pm 13}{21}$	$\frac{25 \pm 20}{22}$	$\frac{41 \pm 33}{24}$	$\frac{145 \pm 104}{13}$
AN <sub>0</sub>	$\frac{0.93 \pm 0.48}{21}$	$\frac{0.70 \pm 0.45}{22}$	$\frac{0.86 \pm 0.56}{24}$	$\frac{1.21 \pm 0.61}{17}$
AN <sub>m</sub>	$\frac{1.03 \pm 0.57}{21}$	$\frac{1.09 \pm 1.89}{22}$	$\frac{0.96 \pm 0.60}{24}$	$\frac{1.21 \pm 0.61}{17}$
H <sub>phs</sub>	$\frac{38 \pm 23}{21}$	$\frac{20 \pm 7}{22}$	$\frac{14 \pm 8}{24}$	$\frac{12 \pm 5}{17}$

Areas of different trophic levels are distinguished on the basis of Chl<sub>0</sub> content (mg/m<sup>3</sup>). The numerator shows arithmetic mean values and standard deviation and the denominator shows the number of measurements. Designations of indices: Chl<sub>0</sub>—the concentration of Chl on the surface, mg/m<sup>3</sup>; Chl<sub>phs</sub>, Chl<sub>1.5phs</sub>, Chl<sub>Z</sub>, and Chl<sub>UML</sub>—the total chlorophyll content (mg/m<sup>2</sup>) in the photosynthetic layer, in the layer of 1.5H<sub>phs</sub>, in layer Z (1/k<sub>d</sub>) (for explanations, see text), and in the upper mixed layer, respectively; PP<sub>0</sub>—primary production on the surface, mg C/m<sup>3</sup> per day; PP<sub>phs</sub>, PP<sub>Z</sub>, and PP<sub>UML</sub>—integrated primary production (mg C/m<sup>2</sup> per day) in the euphotic layer, in layer Z, and in the upper mixed layer, respectively; AN<sub>0</sub> and AN<sub>m</sub>—surface and maximum assimilation numbers (mg C/mg Chl *a* per hour), respectively; and H<sub>phs</sub>—photosynthetic layer thickness, m.

expressed SCM, the vertical distribution of Chl can be described by three types of curves (Fig. 1). In the open shelf of the southwestern area (> 100 m), maximum Chl was detected on the surface; its content gradually decreased in the layer of maximum gradients of the pycnocline and remained practically unchanged beneath this layer. In the mouth of estuaries, the Chl concentration was uniformly distributed in the layer from the surface to the bottom, whereas in the middle of the estuarine area its content did not change in the UML and sharply decreased below this layer (Fig. 1).

The SCM was formed usually in the layer of maximum gradients of the pycnocline or immediately beneath the latter at horizons where an increase of the content of NO<sub>2</sub> + NO<sub>3</sub> was observed (Fig. 2).

Curves showing the vertical distribution of PP were more uniform as compared to the Chl profiles. The PP maximum was recorded on the surface or in the layer 0–5 m. Below this layer, PP values decreased with depth (Fig. 1). Exceptions to this trend were some stations with a distinct SCM, at which a secondary PP maximum was formed in this layer (Fig. 2). The depth

**Table 2.** Values of some abiotic factors in the Kara Sea waters of different trophic levels

Index	Trophic level			
	0.1–0.5	0.5–1.0	1.0–2.0	>2.0
$k_d$	$\frac{0.210 \pm 0.147}{25}$	$\frac{0.308 \pm 0.062}{30}$	$\frac{0.447 \pm 0.129}{36}$	$\frac{0.582 \pm 0.132}{19}$
$Z$	$\frac{5 \pm 1}{25}$	$\frac{3 \pm 1}{30}$	$\frac{2 \pm 1}{36}$	$\frac{2 \pm 1}{19}$
10%	$\frac{12 \pm 3}{25}$	$\frac{8 \pm 2}{30}$	$\frac{6 \pm 1}{36}$	$\frac{4 \pm 1}{19}$
1%	$\frac{23 \pm 5}{25}$	$\frac{16 \pm 4}{30}$	$\frac{11 \pm 3}{36}$	$\frac{8 \pm 3}{19}$
0.1%	$\frac{35 \pm 8}{25}$	$\frac{23 \pm 5}{30}$	$\frac{17 \pm 5}{36}$	$\frac{13 \pm 4}{19}$
$I_0$	$\frac{7.32 \pm 4.43}{23}$	$\frac{4.16 \pm 2.53}{16}$	$\frac{4.60 \pm 3.48}{15}$	$\frac{8.86 \pm 8.07}{16}$
$PO_{4av}$	$\frac{0.30 \pm 0.26}{18}$	$\frac{0.26 \pm 0.18}{22}$	$\frac{0.50 \pm 0.36}{21}$	$\frac{0.63 \pm 0.59}{16}$
$NO_2 + NO_{3av}$	$\frac{1.58 \pm 1.55}{21}$	$\frac{0.97 \pm 1.18}{22}$	$\frac{1.45 \pm 1.67}{21}$	$\frac{1.81 \pm 1.59}{17}$
$Si(OH)_{4av}$	$\frac{3.88 \pm 3.53}{21}$	$\frac{8.11 \pm 7.92}{22}$	$\frac{23.67 \pm 16.68}{21}$	$\frac{50.18 \pm 36.08}{17}$
$NH_{4av}$	$\frac{0.64 \pm 0.37}{13}$	$\frac{0.75 \pm 0.40}{22}$	$\frac{0.92 \pm 0.49}{16}$	$\frac{1.79 \pm 1.19}{15}$
$\Delta\sigma_t (\sigma_{t20} - \sigma_{t0})$	$\frac{14.82 \pm 19.78}{24}$	$\frac{21.44 \pm 23.62}{19}$	$\frac{21.19 \pm 21.28}{32}$	$\frac{19.12 \pm 15.17}{15}$
UML	$\frac{10 \pm 5}{25}$	$\frac{8 \pm 4}{30}$	$\frac{7 \pm 3}{36}$	$\frac{10 \pm 7}{20}$

Areas of different trophic levels were distinguished on the basis of  $Chl_0$  content ( $mg/m^3$ ). The numerator shows the arithmetic mean values and the standard deviation and the denominator shows the number of measurements. Designations of indices:  $k_d$ —coefficient of diffuse attenuation of PAR,  $m^{-1}$ ;  $Z$ —thickness of the layer generating integrated flux of upward radiation in the PAR range, recorded with a satellite color scanner ( $1/k_d$ ), m; 10%, 1%, and 0.1%—penetration depths of the subsurface PAR, m;  $I_0$ —subsurface irradiance in the PAR range,  $Ein/m^2$  per day;  $PO_{4av}$ ,  $NO_2 + NO_{3av}$ ,  $Si(OH)_{4av}$ , and  $NH_{4av}$ —average content of phosphates, sum of nitrites and nitrates, dissolved silica, and ammonium nitrate, respectively, in the photosynthetic layer,  $\mu M$ ;  $\Delta\sigma_t (\sigma_{t20} - \sigma_{t0})$ —the water column stability index, calculated as the difference between the densities at depths of 0 and 20 m; and UML—the thickness of the upper mixed layer, m.

of the photosynthetic layer decreased, on average, from 38 to 12 m upon the transition from waters of type I to type IV (Table 1).

For a more complete understanding of the conditions of depth-integrated PP formation, it is expedient to present an averaged picture of vertical changes in PP and Chl in the Kara Sea regions with different productivity levels (Fig. 3). The average values of PP and Chl were calculated within each trophic category for 5-m layers of water of the upper 55 m. An averaged picture of the vertical distribution of Chl indicates that

the SCM in the waters of the Kara Sea in autumn is poorly expressed. In the waters of trophic type I ( $Chl_0 = 0.1\text{--}0.5 mg/m^3$ ), in the layer of 20–25 m, a slight SCM ( $Chl_m/Chl_0 = 1.25$ ) was recorded. The  $I_0$  value in this layer was close to 1% of subsurface PAR (Fig. 3). In the waters of trophic types II–IV, the mean Chl content uniformly decreased with depth. The PP maximum was recorded on the surface, and a secondary peak for these trophic categories was not distinct. The same conclusion can be made for the vertical distribution of the assimilation number. Optimal assimi-

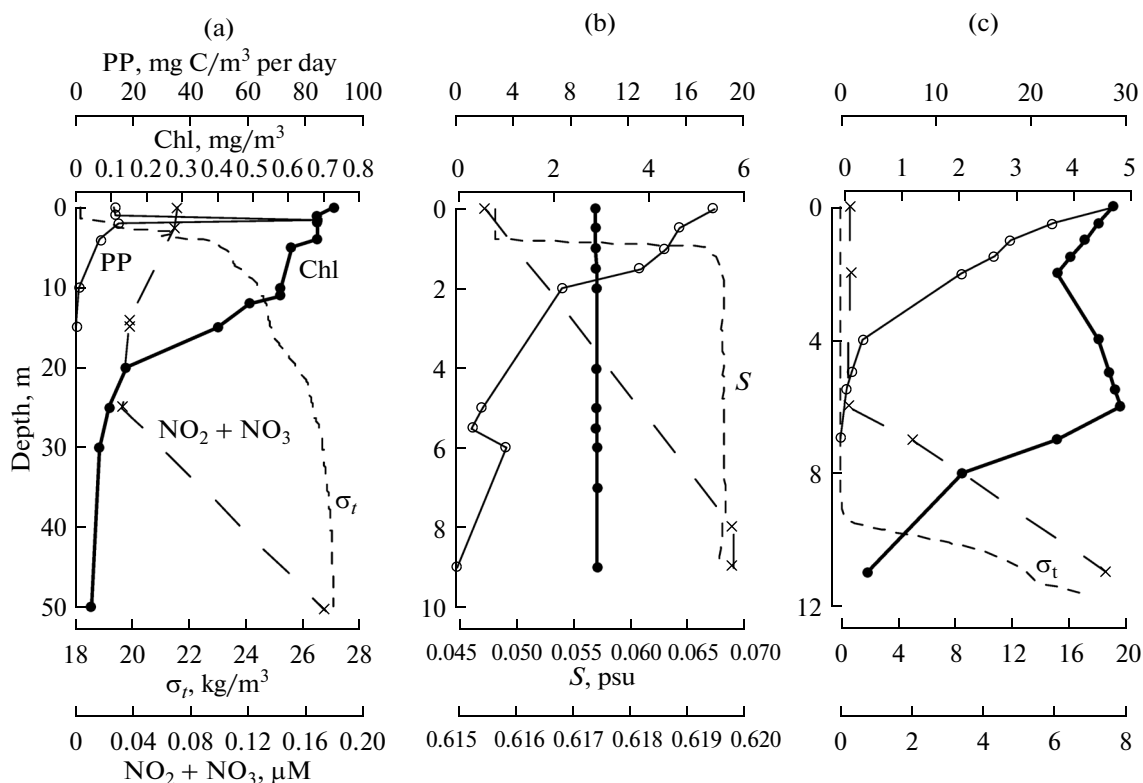


**Fig. 1.** Vertical distribution of the primary production (PP), chlorophyll (Chl), the sum of nitrite and nitrate ( $\text{NO}_2 + \text{NO}_3$ ), salinity ( $S$ ), and water density ( $\sigma_t$ ) in the Kara Sea at stations without a strong chlorophyll maximum: (a) September 15, 2011, south-western region, depth 138 m,  $72^\circ 20' \text{ N}$ ,  $65^\circ 58' \text{ E}$ ; (b) September 19, 2011, near-mouth area of the Yenisei River estuary, depth 13 m,  $71^\circ 52' \text{ N}$ ,  $82^\circ 12' \text{ E}$ ; (c) September 19, 2011, central part of the Yenisei River estuary, depth 13 m,  $72^\circ 10' \text{ N}$ ,  $81^\circ 00' \text{ E}$ .

lation activity of phytoplankton was recorded at different stations within the upper 5-m layer. It should be noted that the average curves of the vertical distribution of Chl do not always characterize the picture for some stations (Figs. 1, 2).

**Layered distribution of primary production and chlorophyll in the waters of different trophic levels.** Table 3 shows the results of evaluation of the contribution of different layers to the integrated PP and Chl values. Of interest to us were layers  $Z$ , which generates a signal for the satellite color scanner ( $1/k_d$ ), UML, and the layer below the photosynthetic layer ( $H_{1.5\text{phs}} - H_{\text{phs}}$ ). The integrated PP values in layer  $Z$  consistently increased as water productivity increased from 43 to 53% of  $\text{PP}_{\text{phs}}$ . The integrated Chl content in this layer ( $\text{Chl}_z$ ) increased from 16%  $\text{Chl}_{\text{phs}}$  in the waters of trophic level I to 28% in type III waters. For  $\text{Chl}_0$  values  $> 2 \text{ mg/m}^3$ , the contribution of  $\text{Chl}_z$  reduced to 21%, which can be explained by a decrease in the thickness of layer  $Z$  in estuarine waters with a high content of particulate and dissolved matter (Table 2). In the upper mixed layer, integrated PP and Chl values consistently increased with increases in the trophic level of waters. The contribution of UML to  $\text{PP}_{\text{phs}}$  and  $\text{Chl}_{\text{phs}}$  changed from 60 to 88% and from 30 to 67%, respectively. The Chl content below the photosyn-

thetic layer ranged from 17 to 22% and hardly changed when the trophic level changed (Table 3).

## DISCUSSION

**Characteristics of vertical distribution of Chl: the formation of SCM and its effect on the primary production in the water column.** A common feature of the vertical distribution of Chl in stratified waters of the first optical type (Case I) is the formation of the SCM and an increase in its depth with a decrease in the Chl concentration on the surface [36, 53]. Our study showed that this pattern is also observed in waters of the second optical type (Case II) with a high concentration of particulate and dissolved matter, to which the majority of areas of the Kara Sea belong. The available data did not allow us to distinguish water areas with a  $\text{Chl}_0$  content  $< 0.1 \text{ mg/m}^3$ , and the question of the shape of the curve of the vertical distribution of Chl in the waters of the Kara Sea under conditions of oligotrophy remains open.

The analysis of the average curves of the vertical distribution of Chl in the waters of different trophic levels suggests that the SCM in the Kara Sea is weak and is observed mainly in the  $\text{Chl}_0$  content from 0.1 to  $0.5 \text{ mg/m}^3$  (68% of stations) and that the Chl maxi-

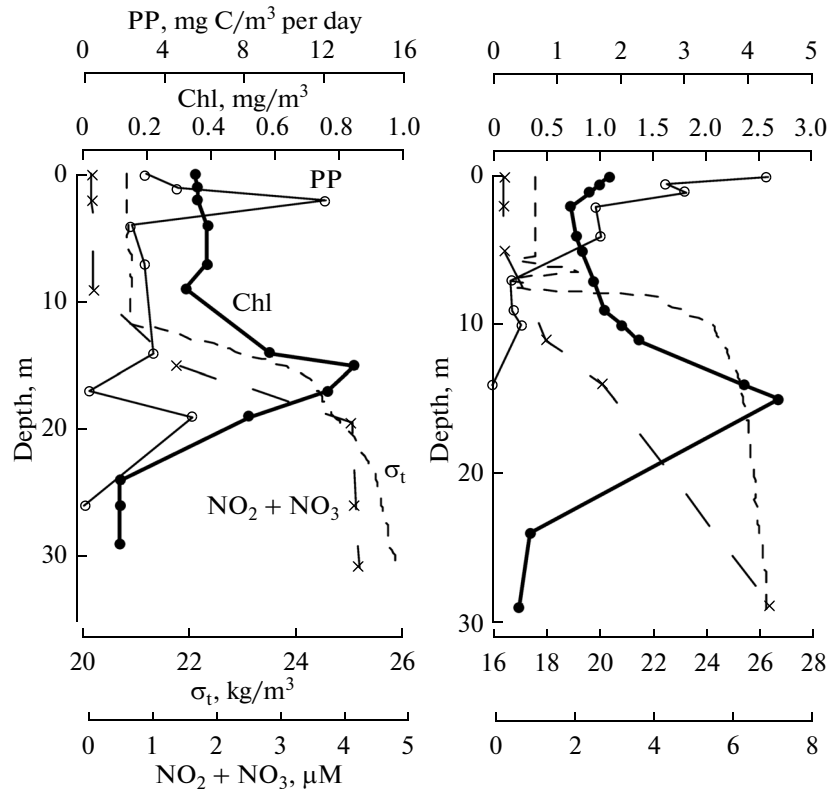


**Fig. 2.** Vertical distribution of primary production (PP), chlorophyll (Chl), sum of nitrite and nitrate ( $\text{NO}_2 + \text{NO}_3$ ), and water density ( $\sigma_t$ ) in the Kara Sea at stations with a strong chlorophyll maximum: (a) September 17, 2011, shelf area, depth 32 m,  $74^\circ 17' \text{ N}$ ,  $78^\circ 37' \text{ E}$ ; (b) September 20, 2011, shelf area, depth 29 m,  $73^\circ 43' \text{ N}$ ,  $79^\circ 24' \text{ E}$ .

imum is usually detected on the surface (Fig. 4). The number of stations with a strong SCM decreased with increasing water productivity (Table 4) [19]. The weak expression of  $\text{Chl}_m$  after averaging the vertical profiles can be explained by both the variability of depths where SCM is recorded and the high variability of Chl values in the water column. Table 4 shows, in general, that, as  $\text{Chl}_0$  increased, the depths where SCM was detected decreased, whereas the  $\text{Chl}_m$  value, conversely, increased. Earlier, the same pattern was observed for the tropical and temperate latitudes of the World Ocean [36, 53] and for the Arctic Ocean [8]. The thickness of the SCM was maximum in waters of trophic type I (on average, 13 m) and changed slightly as the productivity of waters increased, whereas the degree of manifestation of the SCM ( $\text{Chl}_m/\text{Chl}_0$ ) in general decreased. It should be noted that, in waters with  $\text{Chl}_0 > 1 \text{ mg/m}^3$  (types III and IV), the SCM was manifested only at three stations (Table 4).

The nature of the vertical distribution of Chl (in particular, the presence of SCM) in the Arctic Ocean may have a significant effect on annual depth-integrated PP, accounting for 65–90% of its value [38]. The SCM can be formed immediately after ice breakup [40–42, 52] and in summer after the bloom; it may promote the formation of secondary peaks of PP or attenuate the effect of reducing the PP with increasing depth [8, 11, 39]. The results of previous

calculations showed that, in the Kara Sea, the contribution of PP to the SCM layer in waters of different trophic levels varied from 1 to 27% [19]. This estimate is relevant for the use of vertical curves of Chl in PP models of the Arctic seas [8, 11]. Interestingly, the contribution of the Chl maximum to integrated Chl values in the study layer hardly changed (Table 4). Our results were close to estimates of the contribution of the SCM to  $\text{PP}_{\text{phs}}$  obtained earlier in September for Baffin Bay (5.1–15.8%), the Beaufort Sea (20.4%), and the Greenland Sea (16.6%) [8].

The characteristics of the vertical distribution of Chl in the Kara Sea are reflected in the pattern of  $\text{Chl}_0$  dependence on  $\text{Chl}_{\text{phs}}$  [19]. The weak correlation between these parameters ( $R^2 = 0.22$ ) confirms the conclusion that the production characteristics of the surface layer of the Kara Sea do not adequately characterize the integrated values. In the Kara Sea [19], the  $\text{Chl}_{\text{phs}}$  value is always less than those in the other regions of the World Ocean with the same  $\text{Chl}_0$  concentrations [36, 53]. As was noted recently by Ardina et al., the correlation between  $\text{Chl}_0$  and  $\text{Chl}_{\text{phs}}$  in the Arctic Ocean decreases during the year, reaching minimum values after the bloom, which may be caused by the formation of SCM during this period [8].

In order to determine consistent patterns of SCM in the Kara Sea, it is necessary to consider correlations

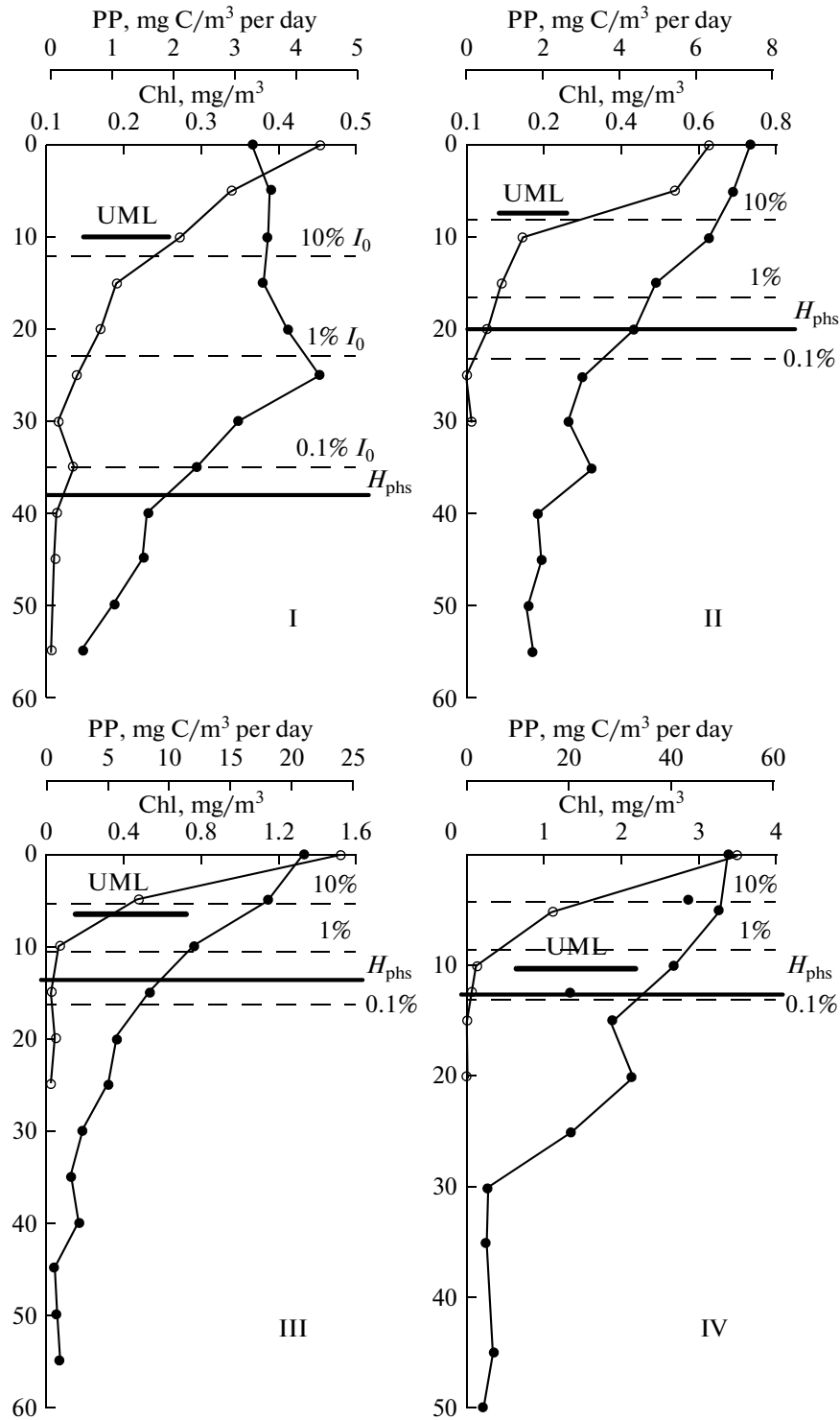


**Fig. 3.** Averaged profiles of the vertical distribution of the primary production (PP) and chlorophyll (Chl), the average position of the boundary of the upper mixed layer (UML), and the photosynthetic layer ( $H_{\text{phs}}$ ), as well as 10, 1, and 0.1% levels of subsurface irradiance in the PAR range ( $I_0$ ) in waters of the Kara Sea with a  $\text{Chl}_0$  content of (I) 0.1–0.5 mg/m<sup>3</sup>, (II) 0.5–1.0 mg/m<sup>3</sup>, (III) 1.0–2.0 mg/m<sup>3</sup>, and (IV) > 2 mg/m<sup>3</sup>.

**Table 3.** Relative distribution of primary production (PP) and chlorophyll (Chl) in layer Z, UML, and below the photosynthetic layer (for explanations, see the text) in the Kara Sea waters of different trophic levels

Trophic level	Layer, m				
	$Z (1/k_d)$		UML		$H_{1.5\text{phs}} - H_{\text{phs}}$
	% of the integrated value in the photosynthetic layer				
	Chl	PP	Chl	PP	$\Delta\text{Chl} = (\sum\text{Chl}_{1.5\text{phs}} - \text{Chl}_{\text{phs}}) / \sum\text{Chl}_{1.5\text{phs}}$
0.1–0.5	16	43	30	60	20
0.5–1.0	25	47	51	66	20
1.0–2.0	28	52	58	78	17
>2.0	21	53	67	88	22

Areas of different trophic levels were distinguished on the basis of  $\text{Chl}_0$  content ( $\text{mg}/\text{m}^3$ ). Designations of indices:  $H_{1.5\text{phs}} - H_{\text{phs}}$ —the layer located between the boundaries of the photosynthetic layer and the study layer, m;  $\Delta\text{Chl}$ —relative Chl content below the photosynthetic layer, %. For other designations, see the text and the notes to Table 2.

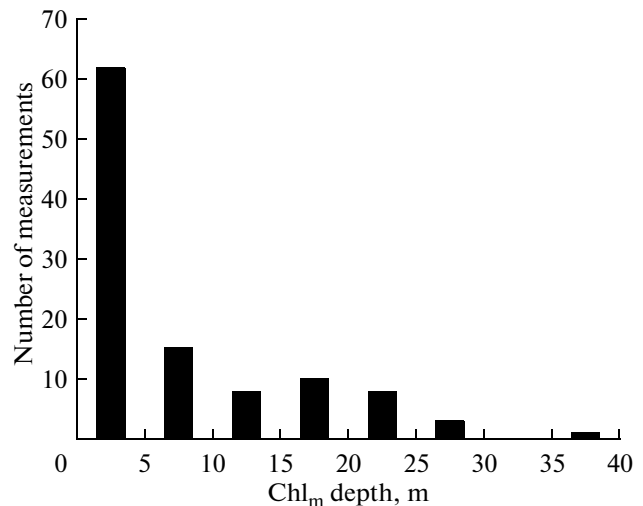
between depths where SCM is detected and abiotic factors. As can be seen in Fig. 5, the depth of SCM approximately equally depended on the optical (1% level of PAR and  $k_d$ ), hydrophysical (UML thickness), and hydrochemical (nutricline depth ( $H_{\text{nut}}$ )) parameters. On the basis of these data, it can be concluded that the SCM in the Kara Sea is apparently formed in accordance with the general patterns characteristic of the Arctic Ocean—at the upper nutricline boundary at an irradiance that is still sufficient for photosynthesis (approximately 1% of PAR) [9, 21, 25, 39, 45, 52]. This process is observed after the bloom, when the reserves of biogenic elements in the UML are exhausted. In oligotrophic areas of the World Ocean, the formation of SCM is often associated with an increase in the Chl content in phytoplankton cells due to photoadaptation to a low irradiance [18, 20, 30].

The relative position of the curves for PP and  $\text{NO}_2 + \text{NO}_3$  show that the upper nutricline boundary was located within the photosynthetic layer or close to its lower boundary (Figs. 1, 2) and that the depth at which the SCM was observed directly depended on the thickness of the photosynthetic layer (Fig. 5). It should be noted that the  $\text{NO}_2 + \text{NO}_3$  concentration in the nutricline in some stations may be below values that are limiting for photosynthesis ( $<2 \mu\text{M}$ ) [22], which may prevent SCM formation. In addition to  $H_{\text{nut}}$  and irradiance, the formation of subsurface Chl maximum in the Kara Sea is closely associated with water-column stability, as indicated by the relatively high correlation between SCM and UML thickness ( $R = 0.64$ ) (Fig. 5), in contrast to other regions of the Arctic Ocean, where the SCM can often be located below the UML [39].

Thus, a complex of factors may affect SCM formation in the Kara Sea in summer and autumn. The equivalent influence of several abiotic factors on the SCM formation can be due to the presence of strong stratification and low water transparency, which lead to a shallow nutricline position and a small photosyn-

thetic layer thickness. In this case, the distinction of the dominant factor is hampered and requires more material. It can only be assumed that, similar to the World Ocean, a decrease in the trophic level of waters should lead to an increase in the depth at which the SCM is observed and, respectively, to deepening of  $H_{\text{nut}}$  and 1% PAR.

Previous studies have shown that the presence of SCM in the Arctic Ocean is a characteristic feature of the vertical distribution of phytoplankton in the ice-free period of the year [12, 26, 37, 39, 52]. In the World Ocean, SCM is typically present in the stratified waters of optical type I, and the degree of its manifestation depends on the level of productivity, an indicator of which is the  $\text{Chl}_0$  content [36, 53]. In the Arctic Ocean, the absence of SCM was observed near the confluence of rivers and in shallow stations ( $< 100 \text{ m}$ ) at vigorous mixing [39]. In Greenland and the Norwe-

**Fig. 4.** Distribution of frequencies of depths where chlorophyll maximum ( $\text{Chl}_m$ ) is observed.

**Table 4.** Characteristics of the chlorophyll maximum in Kara Sea waters of different trophic levels [19]

Trophic level	Number of stations with $Chl_m$	Number of stations with $Chl_m$ , % of the total number	$Chl_m$ layer thickness, m	$Chl_m$ , $mg/m^3$	$Chl_m$ location depth, m	$Chl_m/Chl_0$	$\Sigma Chl_m/\Sigma Chl_{1.5phs}$ , %	$\Sigma PP_m/PP_{phs}$ , %	Number of stations with chlorophyll maximum below $H_{phs}$
0.1–0.5	17	68	$\frac{6-28^{**}}{13}$	$\frac{0.29-1.26}{0.71}$	$\frac{9-40}{20}$	$\frac{1.22-3.56}{2.16}$	$\frac{30-39}{34}$	$\frac{5-46}{23}$	1
0.5–1.0	5	17	$\frac{4-6}{5}$	$\frac{0.71-1.73}{1.06}$	$\frac{8-30}{19}$	$\frac{1.22-1.90}{1.44}$	$\frac{33-40}{35}$	27	3
1.0–2.0	2	6	$\frac{4-5}{5}$	$\frac{2.20-2.68}{2.44}$	$\frac{8-15}{12}$	$\frac{1.51-2.45}{1.98}$	$\frac{33-35}{34}$	$\frac{1-13}{7}$	–
>2.0	1	5	5	2.93	9	1.15	37	1	–

Areas of different trophic levels were distinguished on the basis of  $Chl_0$  content ( $mg/m^3$ ). The numerator shows the limits of the variability of the index, and the denominator shows the arithmetic mean value. Designations of indices:  $Chl_0$  and  $Chl_m$ —the chlorophyll content on the surface and the maximum chlorophyll content in the water column, respectively,  $mg/m^3$ ;  $\Sigma Chl_m$  and  $\Sigma Chl_{1.5phs}$ —integrated Chl values in the maximum layer and in the study layer ( $1.5H_{phs}$ ), respectively ( $mg/m^2$ );  $\Sigma PP_m$  and  $PP_{phs}$ —integrated primary production in the chlorophyll maximum layer and in the photosynthetic layer, respectively ( $mg C/m^2$  per day).

gian Seas, the absence or a shallow (20 m) location of the SCM was also noted, which was explained by the predominance of temperature stratification, in contrast to the majority of other areas of the Arctic, in which halinic stratification dominates [8, 16].

The analysis of available data on the vertical distribution of Chl in the Kara Sea allowed us to conclude that a hydrological and hydrochemical regime favorable for the formation of the SCM only slightly contributes to its formation in autumn. This fact can be explained by the low transparency of water due to the high concentration of particulate and dissolved matter and the low level of available solar radiation at the end of the vegetation season [19]. The presence of the Chl maximum on the surface and the low manifestation of the SCM in the Kara Sea facilitate the estimation of depth-integrated PP on the basis of satellite data using vertical-resolution models.

**Vertical distribution of Chl in the models of integrated primary production in the Kara Sea.** One approach to account for the vertical distribution of Chl in the models of primary production in the Arctic Ocean is to assume

the homogeneous Chl distribution within the UML and an exponential decrease below this layer [43]. In another approach, in addition to the vertical distribution curve of this type, a homogeneous distribution of Chl up to the euphotic zone boundary is assumed [28]. Such curves, in general, describe the vertical structure of the phytoplankton communities in the Arctic Ocean in winter and spring. In general, errors in the estimates of PP in the Arctic Ocean, caused by the omission of subsurface Chl maximum formed after bloom, increase from 0.2% in January to 16% in July and account for, on average, approximately 8% for the annual  $PP_{phs}$ . For oligotrophic areas (Beaufort Sea) it was noted that the contribution of the SCM to the annual depth-integrated primary production may be significant (65–90%) [38]. When using satellite data, the underestimation of PP due to SCM is smoothed by the overestimation of the  $Chl_0$  content (calculated on the basis of indirect optical data obtained with an ocean color scanner), which is determined by the high concentration of dissolved organic matter in the Case II waters of the Arctic Ocean. The total error in this case is < 1% of annual PP in the entire Arctic basin [11]. The same error was cal-

**Fig. 5.** Dependence of the depth where the chlorophyll maximum is observed ( $H_{Chl_m}$ ) on (a) the depth of 1% level of subsurface irradiance in the PAR range, (b) photosynthetic layer thickness ( $H_{phs}$ ), (c) depth of upper nutricline boundary ( $H_{nut}$ ), (d) thickness of upper mixed layer (UML), and (e) diffuse light attenuation coefficient ( $k_d$ ). Stations excluded from the analysis were located in estuarine waters with an abnormally low transparency and a strong freshening of the narrow surface layer.

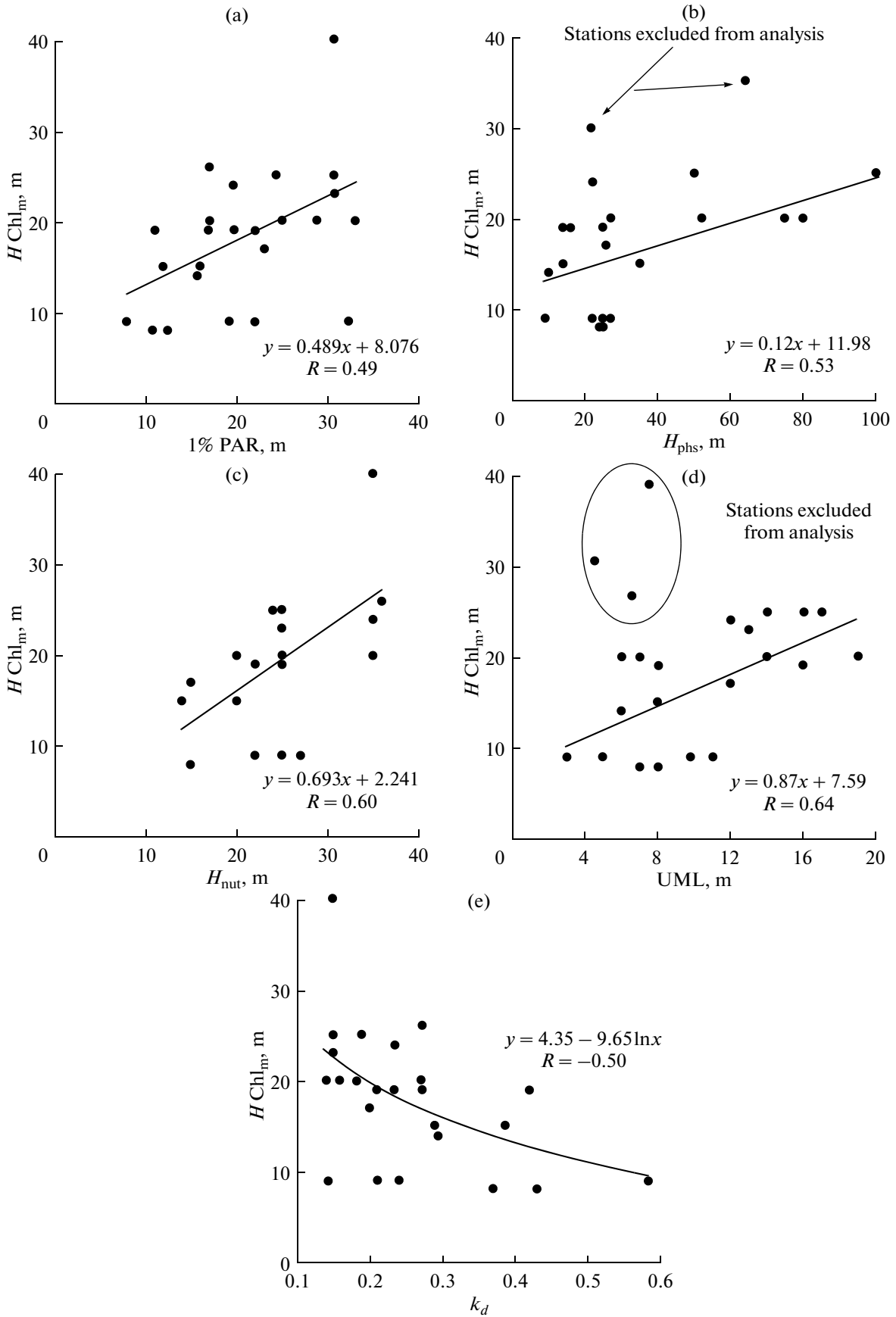


**Table 5.** Parameters of dependences  $y = a + bx$  and  $y = a + b \ln x$  of chlorophyll concentration values normalized to the maximum value in the photosynthetic layer ( $\text{Chl}_{\text{rel}} = \text{Chl}_z / \text{Chl}_m$ ) on the optical depth ( $\zeta$ )

Trophic layer	$x$	$y$	$a$	$b$	$R^2$
0.1–0.5 (within the euphotic layer)	$\zeta$	$\text{Chl}_{\text{rel}}$	–68.96	105.02	0.65
0.1–0.5 (below the euphotic layer)	$\zeta$	$\text{Chl}_{\text{rel}}$	–19.95	17.47	0.89
0.5–1.0	$\zeta$	$\ln \text{Chl}_{\text{rel}}$	–0.08	–8.90	0.92
1.0–2.0	$\zeta$	$\ln \text{Chl}_{\text{rel}}$	0.05	–6.52	0.93
>2.0	$\zeta$	$\text{Chl}_{\text{rel}}$	18.02	–20.20	0.96

Trophic levels were distinguished on the basis of the  $\text{Chl}_0$  content ( $\text{mg}/\text{m}^3$ ).

Designations:  $y$ —dependent variable,  $x$ —independent variable,  $a$  and  $b$ —coefficients in the regression equation, and  $R^2$ —the coefficient of determination.

culated for the Kara Sea, although data for the eastern Arctic Ocean are scarce [10]. Apparently, the correct account of the vertical distribution of Chl in PP models should assume, first, a regional approach and, second, differentiation of Chl curves in waters of different productivity.

This is the first study to perform parameterization of the vertical profiles of Chl in the Kara Sea for their further use in models for calculating the integrated primary production on the basis of satellite data. One approach in this analysis is to obtain the average normalized profiles of PP and Chl for waters with different trophic status. As can be seen from Table 5, vertical profiles of Chl are approximated to high coefficients of determination, linearly in type I and IV waters and exponentially for type II and III waters. Interestingly, at  $\text{Chl}_0$  values  $> 0.5 \text{ mg}/\text{m}^3$ , the Chl content decreases continuously with depth, and only at relatively low surface Chl concentrations ( $0.1\text{--}0.5 \text{ mg}/\text{m}^3$ ) remains close to constant in the euphotic layer (Fig. 3). The principal point is that the Chl maximum is detected either on the surface (types II–IV) or subsurface (type I) layers, i.e.,  $\text{Chl}_m \approx \text{Chl}_0$ . This picture of the vertical distribution of Chl, obtained on a regional scale, is different from the commonly accepted notions taken into account when evaluating  $\text{PP}_{\text{phs}}$  in other water areas of the Arctic and the Arctic Ocean in general [28, 43].

When calculating  $\text{PP}_{\text{int}}$  on the basis of satellite data, to move from the relative values and optical depth to absolute Chl values in horizons and geometric depth,  $\text{Chl}_0$  and  $k_d$  values are required. It should be noted that, in model calculations, the value of Chl in the layer forming the upward radiation signal ( $1/k_d$ ) is used. Regression analysis showed that the mean Chl value in the Kara Sea in the  $1/k_d$  layer is well correlated with the surface Chl value ( $R^2 = 0.99$ , slope = 0.98,  $N = 104$ ) [19]. Thus, vertical profiles of Chl can be deduced using  $k_d$  and  $\text{Chl}_0$  values. At the next step, calculation of PP, satellite data on incoming solar radiation and the dependence of the assimilation number (AN) on the subsurface irradiance in the PAR range are required.

## ACKNOWLEDGMENTS

This study was supported by the Russian Science Foundation (project no. 14-17-00681), the Russian Foundation for Basic Research (project nos. 13-05-00029 and 14-05-05003), and Program 23 of the Presidium of the Russian Academy of Sciences (project no. 9.5).

## REFERENCES

1. V. I. Burenkov, Y. A. Goldin, and M. D. Kravchishina, "The distribution of the suspended matter concentration in the Kara Sea in September 2007 based on ship and satellite data," *Oceanology* (Engl. Transl.) **50** (5), 798–800 (2010).
2. A. S. Bychkov, G. Yu. Pavlova, and V. A. Kropotov, "Carbonate system," in *Chemistry of the Sea Water and Autogenic Mineral Formation* (Nauka, Moscow, 1989), 49–111 [in Russian].
3. V. I. Vedernikov, A. B. Demidov, and A. I. Sud'bin, "Primary production and chlorophyll in the Kara Sea in September 1993," *Okeanologiya* (Moscow) **34** (5), 693–703 (1994).
4. O. A. Kuznetsova, O. V. Kopelevich, S. V. Sheberstov, et al., "Assessment of chlorophyll concentration in the Kara Sea based on the data of satellite scanner MODIS–AQUA," *Issled. Zemli Kosmosa*, No. 5, 21–31 (2013).
5. S. A. Mosharov, "Distribution of the primary production and chlorophyll a in the Kara Sea in September of 2007," *Oceanology* (Engl. Transl.) **50** (6), 884–892 (2010).
6. *Handbook on Chemical Analysis of Sea Water, RD 52.10.242-92* (Gidrometeoizdat, St. Petersburg, 1993) [in Russian].
7. *Modern Hydrochemical Analysis of Ocean*, Ed. by O. K. Bordovskii and V. N. Ivanenkov (Shirshov Scientific Research Institute of Oceanology, Academy of Sciences of Soviet Union, Moscow, 1992) [in Russian].
8. M. Ardyna, M. Babin, M. Gosselin, et al., "Parameterization of vertical chlorophyll  $a$  in the Arctic Ocean: impact of the subsurface chlorophyll maximum on regional, seasonal and annual primary production estimates," *Biogeosciences* **10** (3), 1345–1399 (2013).

9. M. Ardyna, M. Gosselin, C. Michel, et al., "Environmental forcing of phytoplankton community structure and function in the Canadian High Arctic: contrasting oligotrophic and eutrophic regions," *Mar. Ecol.: Progr. Ser.* **442**, 37–57 (2011).
10. K. R. Arrigo and G. L. van Dijken, "Secular trends in Arctic Ocean net primary production," *J. Geophys. Res., C: Oceans Atmos.* **116**, 09011 (2011). doi 10.1029/2011JC007151
11. K. R. Arrigo, P. A. Matrai, and G. L. van Dijken, "Primary productivity in the Arctic Ocean: impacts of complex optical properties and subsurface chlorophyll maxima on large scale estimates," *J. Geophys. Res., C: Oceans Atmos.* **116**, 11022 (2011). doi 10.1029/2011JC007273
12. B. C. Booth, P. Larouche, S. Belanger, et al., "Dynamics of *Chaetoceros socialis* in the north water," *Deep Sea Res., Part II* **49** (22–23), 5003–5025 (2002).
13. J. Campbell, D. Antoine, R. Armstrong, et al., "Comparison of algorithms for estimating ocean primary production from surface chlorophyll, temperature and irradiance," *Global Biogeochem. Cycles* **16** (3), (2002). doi 10.1029/2001GB001444
14. M.-E. Carr, M. A. M. Friedrichs, M. Schmeltz, et al., "A comparison of global estimates of marine primary production from ocean color," *Deep Sea Res., Part II* **53** (5–7), 741–770 (2006).
15. E. C. Carmack, R. W. Macdonald, and S. Jasper, "Phytoplankton productivity on the Canadian shelf of the Beaufort Sea," *Mar. Ecol.: Progr. Ser.* **277**, 37–50 (2004).
16. E. C. Carmack and P. Wassmann, "Food webs and physical-biological coupling on pan-Arctic shelves: unifying concepts and comprehensive perspectives," *Progr. Oceanogr.* **71**, 446–477 (2006).
17. G. F. Cota, L. R. Pomeroy, W. G. Harrison, et al., "Nutrients, primary production, and microbial heterotrophy in the southeastern Chukchi Sea: Arctic summer nutrient depletion and heterotrophy," *Mar. Ecol.: Progr. Ser.* **135**, 247–258 (1996).
18. J. J. Cullen, "The deep chlorophyll maximum: comparing vertical profiles of chlorophyll *a*," *Can. J. Fish. Aquat. Sci.* **39**, 791–803 (1982).
19. A. B. Demidov, S. A. Mosharov, and P. N. Makkaveev, "Patterns of the Kara Sea primary production in autumn: biotic and abiotic forcing of subsurface layer," *J. Mar. Syst.* **132**, 130–149 (2014).
20. K. Fennel and E. Boss, "Subsurface maxima of phytoplankton and chlorophyll: steady-state solutions from a simple model," *Limnol. Oceanogr.* **48** (4), 1521–1534 (2003).
21. J. Ferland, M. Gosselin, and M. Starr, "Environmental control of summer primary production in the Hudson Bay system: the role of stratification," *J. Mar. Syst.* **88**, 385–400 (2011).
22. T. R. Fisher, E. R. Peele, J. W. Ammerman, and L. W. J. Harding, "Nutrient limitation of phytoplankton in Chesapeake Bay," *Mar. Ecol.: Progr. Ser.* **82**, 51–63 (1992).
23. M. A. M. Friedrichs, M.-E. Carr, R. T. Barber, et al., "Assessing the uncertainties of model estimates of primary productivity in the tropical Pacific Ocean," *J. Mar. Syst.* **76** (1–2), 113–133 (2009).
24. H. G. Gordon and A. Morel, *Remote Assessment of Ocean Color for Interpretation of Satellite Visible Imagery: A Review* (Springer-Verlag, New York, 1983).
25. V. Hill and G. Cota, "Spatial patterns of primary production on the shelf, slope and basin of the Western Arctic in 2002," *Deep Sea Res., Part II* **57** (24–26), 3344–3354 (2005).
26. V. Hill, G. Cota, and D. Stockwell, "Spring and summer phytoplankton communities in the Chukchi and Eastern Beaufort Seas," *Deep Sea Res., Part II* **52** (24–26), 3369–3385 (2005).
27. V. J. Hill, P. A. Matrai, E. Olson, et al., "Synthesis of integrated primary production in the Arctic Ocean: II. In situ and remotely sensed estimates," *Progr. Oceanogr.* **110**, 107–125 (2013).
28. V. J. Hill and R. C. Zimmerman, "Estimates of primary production by remote sensing in the Arctic Ocean: Assessment of accuracy with passive and active sensors," *Deep Sea Res., Part I* **57** (10), 1243–1254 (2010).
29. O. Holm-Hansen and B. Riemann, "Chlorophyll *a* determination: improvements in methodology," *Oikos* **30**, 438–447 (1978).
30. J. Huisman, N. N. Pham Thi, D. M. Karl, and B. Sommeijer, "Reduced mixing generates oscillation and chaos in the oceanic deep chlorophyll maximum," *Nature* **439**, 322–325 (2006).
31. H. G. Jerlov, *Optical Oceanography* (Elsevier, New York, 1968).
32. *Protocols for the Joint Global Ocean Flux Study Protocols (JGOFS). Core Measurements, Manual Guides* (UNESCO, 1994), pp. 119–122.
33. S. W. Jeffrey and G. F. Humphrey, "New spectrophotometric equations for determining chlorophylls *a*, *b*, *c1* and *c2* in higher plants, algae and natural phytoplankton," *Biochem. Physiol. Pflanz.* **167** (2), 191–194 (1975).
34. P. N. Makkaveev, "The total alkalinity in the anoxic waters of the Black sea and in sea-river mixture zones," in *Joint IOC-JGOFS CO<sub>2</sub> Advisory Panel Meeting, Seven Session, Annex V* (Intergovernmental Oceanographic Commission, UNESCO, 1998).
35. F. J. Millero, "Thermodynamics of the carbon dioxide system in oceans," *Geochim. Cosmochim. Acta* **59** (4), 661–677 (1995).
36. A. Morel and J.-F. Berthon, "Surface pigments, algal biomass profiles, and potential production of the euphotic layer: relationships reinvestigated in view of remote-sensing applications," *Limnol. Oceanogr.* **34** (1), 1545–1562 (1989).
37. F. A. McLaughlin and E. C. Carmack, "Deepening of the nutricline and chlorophyll maximum in the Canada basin interior, 2003–2009," *Geophys. Res. Lett.* **37**, 24602 (2010). doi 10.1029/2010GL045459
38. J. Martin, D. Dumont, and J.-E. Tremblay, "Contribution of subsurface chlorophyll maxima to primary production in the coastal Beaufort Sea (Canadian Arctic): a model assessment," *J. Geophys. Res.* **118** (11), 5873–6318 (2013).
39. J. Martin, J.-E. Tremblay, J. Gagnon, et al., "Prevalence, structure, and properties of subsurface chloro-

- phyll maxima in Canadian Arctic waters," *Mar. Ecol.: Progr. Ser.* **412**, 69–84 (2010).
40. J. Martin, J.-E. Tremblay, and N. M. Price, "Nutritive and photosynthetic ecology of subsurface chlorophyll maxima in Canadian Arctic waters," *Biogeosciences* **9** (12), 5353–5371 (2012).
  41. C.-J. Mundy, M. Gosselin, J. Ehn, et al., "Contribution of under-ice primary production to an ice-edge upwelling phytoplankton bloom in the Canadian Beaufort Sea," *Geophys. Res. Lett.* **36**, 17601 (2009). doi 10.1029/12009GL038837
  42. M. Palmer, K. Arrigo, C.-J. Mundy, et al., "Spatial and temporal variation of photosynthetic parameters in natural phytoplankton assemblages in the Beaufort Sea, Canadian Arctic," *Polar Biol.* **34** (12), 1915–1928 (2011).
  43. S. Pabi, G. L. van Dijken, and K. R. Arrigo, "Primary production in the Arctic Ocean, 1998–2006," *J. Geophys. Res., C: Oceans Atmos.* **113**, 08005 (2008). doi 10.1029/2007/JC004578
  44. T. Platt, S. Sathyendranath, O. Ulloa, et al., "Ocean primary production and available light: further algorithms for remote sensing," *Deep Sea Res., Part I* **35**, 855–879 (1988).
  45. S. R. Rysgaard, T. G. Nielsen, and B. W. Hansen, "Seasonal variation in nutrients, pelagic primary production and grazing in a high-Arctic coastal marine ecosystem, Young Sound, Northeast Greenland," *Mar. Ecol.: Progr. Ser.* **179**, 13–25 (1999).
  46. V. S. Saba, M. A. M. Friedrichs, M.-E. Carr, et al., "Challenges of modeling depth-integrated marine primary productivity over multiple decades: a case study at BATS and HOT," *Global Biogeochem. Cycles* **24** (3), (2010). doi 10.1029/2009GB003655
  47. V. S. Saba, M. A. M. Friedrichs, D. Antoine, et al., "An evaluation of ocean color model estimates of marine primary productivity in coastal and pelagic regions across the globe," *Biogeosciences* **8**, 489–503 (2011).
  48. SCOR–UNESCO, *Report of SCOR–UNESCO Working Group 17 on Determination of Photosynthetic Pigments in Sea Water, Monograph of Oceanography Methodology* (UNESCO, Paris, 1966), Vol. 1, pp. 9–18.
  49. N. E. Steemann, "The use of radioactive carbon ( $C^{14}$ ) for measuring organic production in the sea," *J. Cons. Perm. Ins. Explor. Mer*, No. 18, 117–140 (1952).
  50. J. H. Steele and C. S. Yentsch, "The vertical distribution of chlorophyll," *J. Mar. Biol. Assoc. U.K.* **39**, 217–226 (1960).
  51. G. Tremblay, C. Belzile, M. Gosselin, et al., "Late summer phytoplankton distribution along a 3500 km transect in Canadian Arctic waters: strong numerical dominance by picoeukaryotes," *Aquat. Microb. Ecol.* **54** (1), 55–70 (2009).
  52. J. E. Tremblay, K. Simpson, J. Martin, et al., "Vertical stability and the annual dynamics of nutrients and chlorophyll fluorescence in the coastal, southeast Beaufort Sea," *J. Geophys. Res., C: Oceans Atmos.* **113**, 07S90 (2008). doi 10.1029/2007JC004547
  53. J. Uitz, H. Claustre, A. Morel, and S. B. Hooker, "Vertical distribution of phytoplankton communities in open ocean: an assessment on surface chlorophyll," *J. Geophys. Res., C: Oceans Atmos.* **111**, 08005 (2006). doi 10.1029/2005JC003207

*Translated by M. Batrukova*